Hole concentration in a diluted ferromagnetic semiconductor

Raimundo R dos Santos[1]**, Luiz E Oliveira**[2] **and
J d'Albuquerque e Castro**[1]

[1] Instituto de Física, Universidade Federal do Rio de Janeiro, CP 68.528,
21945-970 Rio de Janeiro RJ, Brazil
[2] Instituto de Física, Unicamp, CP 6165, 13083-970 Campinas SP, Brazil

Abstract
We consider a mean-field approach to the hole-mediated ferromagnetism in
III–V Mn-based semiconductor compounds in order to discuss the dependence
of the hole density on that of Mn sites in $Ga_{1-x}Mn_xAs$. The hole concentration,
p, as a function of the fraction of Mn sites, x, is parametrized in terms of the
product $m^* J_{pd}^2$ (where m^* is the hole effective mass and J_{pd} is the Kondo-
like hole/local-moment coupling), and the critical temperature T_c. By using
experimental data for these quantities, we have established the dependence
of the hole concentration on x, which can be associated with the occurrence
of a re-entrant metal–insulator transition taking place in the hole gas. We
also calculated the dependence of the Mn magnetization on x, for different
temperatures (T), and found that as T increases, the width of the composition-
dependent magnetization decreases dramatically, and that the magnetization
maxima also decrease in magnitude, indicating the need for quality control of
the Mn doping level in diluted magnetic semiconductor devices.

(Some figures in this article are in colour only in the electronic version)

Over the last few decades, a considerable amount of work has been devoted to the understanding
of electronic, optical, and transport properties of diluted magnetic semiconductors (DMS).
Interest in these materials was boosted in the early 1990s by the discovery of ferromagnetism in
III–V materials alloyed with transition elements like Mn [1,2]. Ferromagnetic semiconductors
introduce the possibility of controlling both spin and charge degrees of freedom, which, when
combined with the capability of growing low-dimensional structures, opens up exciting new
prospects for the production of spintronic devices. Potential applications include those in
non-volatile memory systems [3–7] and in quantum computing [8].

Special attention has been focused on $Ga_{1-x}Mn_xAs$ alloys, which exhibit very interesting
magnetic and transport properties. Mn atoms have five electrons in the 3d levels and two

electrons in the 4s levels, and their incorporation into a GaAs matrix plays two roles: they act both as $S = 5/2$ local moments, and as acceptors generating hole states in the material. The equilibrium solubility of Mn atoms in GaAs is quite low, being only of the order of 10^{19} cm^{-3} [9]. However, using molecular-beam epitaxy techniques at low temperatures, several groups have recently succeeded in producing homogeneous samples of Ga$_{1-x}$Mn$_x$As with x as high as 0.071. It has been observed that for $0.015 \leqslant x \leqslant 0.071$ the system becomes ferromagnetic, with a doping-dependent critical temperature $T_c(x)$ reaching a maximum of 110 K for $x = 0.053$ [10].

The appearance of a ferromagnetic state in these materials has been attributed to an exchange coupling between the localized Mn moments mediated by the holes, whose strength should depend on the hole concentration p. In principle, one would expect each Mn to provide one hole, leading to a density of holes equal to that of the magnetic ions. However, while an accurate determination of the hole concentration is hindered by the anomalous Hall term, experimental data indicate that p is only 15–30% of the concentration of magnetic ions [10–13]. The mechanism responsible for the discrepancy between hole and Mn densities is not clear. As pointed out by Matsukura *et al* [11], such a discrepancy might be due to compensation of Mn acceptors by deep donors such as As antisites, which are known to be present at high concentration in low-temperature-grown GaAs [14]. Another possibility is the formation of sixfold-coordinated centres with As (Mn$^{6\text{As}}$), which would compensate Mn atoms on substitutional Ga lattice sites [15]. As a consequence, the relation between the hole concentration and that of Mn has not been so far theoretically established; it would be of great interest for the design of new devices. Our main purpose here is to present a quantitative analysis on this issue, based on a simple model for the magnetic behaviour of these systems.

We adopt the generally accepted view that a given Mn ion interacts with the holes via a local antiferromagnetic Kondo-like exchange coupling J_{pd} between their moments [13, 16–19]. This interaction is thought to lead to the polarization of the hole subsystem, which would then give rise to an effective ferromagnetic coupling between the Mn moments. Though there has been some debate as far as the details of the above picture are concerned (e.g., whether or not such effective interaction is well described by an RKKY term [20, 21]), there is an overall consensus on the fundamental role played by the hole-mediated mechanism. At any rate, the approach we follow here does not depend on the details of the effective Mn–Mn interaction.

We start with a Hamiltonian for the two coupled subsystems of the form

$$\mathcal{H} = \mathcal{H}_{\text{Mn}} + \mathcal{H}_h + J_{pd} \sum_{i,I} \boldsymbol{S}_I \cdot \boldsymbol{s}_i \delta(\boldsymbol{r}_i - \boldsymbol{R}_I), \tag{1}$$

where $\mathcal{H}_{\text{Mn}}$ describes the *direct* (i.e., non-hole-mediated) antiferromagnetic exchange between Mn spins, $\mathcal{H}_h$ describes the hole subsystem, and the last term corresponds to the aforementioned Mn–hole exchange interaction, with $\boldsymbol{S}_I$ and $\boldsymbol{s}_i$ labelling the localized Mn spins ($S = 5/2$) and the hole spins ($s = 1/2$), respectively. As a first approach, we neglect $\mathcal{H}_{\text{Mn}}$ and consider $\mathcal{H}_h$ within a parabolic band effective-mass approximation; we comment below on more general descriptions of $\mathcal{H}_h$.

Within a mean-field approximation, the Mn magnetization is given by

$$M = n_{\text{Mn}} g \mu_{\text{B}} \mathcal{M}_I = n_{\text{Mn}} g \mu_{\text{B}} S B_S \left[\left(\frac{J_{pd} S}{2 k_{\text{B}} T} \right) \mathcal{M}_h \right], \tag{2}$$

where $n_{\text{Mn}} = x n_s$ is the density of Mn ions, with n_s being the density of Ga lattice sites, $\mathcal{M}_I$ is the magnetization density of the Mn ions, $g = 2$ is the Mn Landé g-factor, and $B_S[\cdots]$ is the Brillouin function. The magnetization density of the hole subsystem, $\mathcal{M}_h = \langle n_\uparrow - n_\downarrow \rangle$, is supposed to be uniform within the length scale of magnetic interactions, so it can be calculated
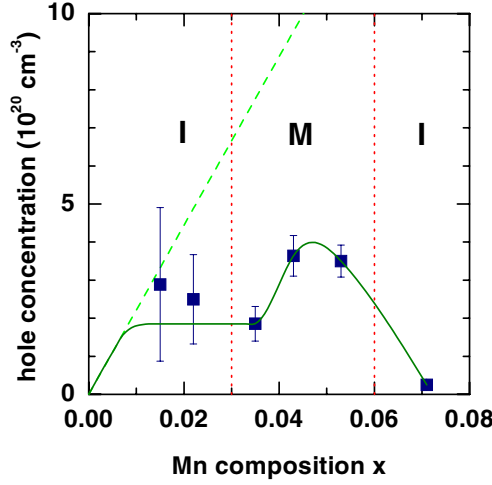
Figure 1. Theoretical results for the hole concentration as a function of the fraction of Mn sites for a (Ga, Mn)As ferromagnetic alloy. The dashed line corresponds to a hole concentration equal to that of the Mn sites, whereas the filled squares are the present mean-field result; the full curve is obtained as explained in the text. I and M respectively denote insulating and metallic phases.

self-consistently by considering a Fermi sea of holes with effective mass m^*, in the presence of the mean magnetic field generated by the Mn ions; it is therefore given by

$$\mathcal{M}_h = \lambda \frac{m^*}{m_e} J_{pd} x \mathcal{M}_I p^{1/3}, \tag{3}$$

where $\lambda = 6(1/3\pi^2)^{2/3}(m_e/\hbar^2 a^3)$, with m_e the free-electron mass; $a = 5.65$ Å is the GaAs lattice constant.

The critical temperature as a function of the hole density and the Mn composition is obtained by linearizing the self-consistency relations given by equations (2) and (3):

$$T_c = \frac{\lambda}{6k_B} S(S+1)[(m^*/m_e) J_{pd}^2] x p^{1/3}. \tag{4}$$

Specializing equation (4) to $S = 5/2$, we write the hole concentration as

$$p = \zeta \left\{ \frac{T_c(x)}{[(m^*/m_e) J_{pd}^2] x} \right\}^3, \tag{5}$$

where $\zeta = 5.29 \times 10^{-16}$, in units such that J_{pd} is given in eV nm^3.

In view of the uncertainty in the available experimental values for m^* and J_{pd}, and to the difficulties in obtaining accurate estimates over a wide range of hole densities, p, the following strategy is adopted. We first use the fact that Hall resistance measurements [22] yield an unambiguous[3] value of $p = 3.5 \times 10^{20}$ cm^{-3} for the sample with $x = 0.053$, for which $T_c = 110$ K. We then put these values into equation (5), giving a value for the product $(m^*/m_e) J_{pd}^2 = 2.4 \times 10^{-2}$ (eV nm^3)^2. And, finally, we use this value, together with the experimental transport data [10] for $T_c(x)$, to obtain p over a wide range of x— shown as filled squares in figure 1. The error bars in figure 1 reflect the uncertainties in the determination of $T_c(x)$, as displayed in figure 3(c) of [10]. The adequacy of this procedure

---

[3] As pointed out in [6], the currently accepted value $p = 3.5 \times 10^{20}$ cm^{-3} is a factor 2.3 larger than the early estimate of [11].

is illustrated in figure 1. The calculated values for $p(x)$ lie below the concentration of Mn ions, shown as a dashed curve, in agreement with experiment. We also highlight in figure 1 the boundaries of the metal–insulator transitions (MITs), as determined from resistivity measurements [10]. The present theoretical estimates for p in the insulating phases are based on the assumption that the localization length in insulating samples, though finite, is significantly larger than the length scale of magnetic interactions [13], in which case the present mean-field approach is a good starting point.

Before accepting these estimates for $p(x)$ at face value, one should note that a closer look at the experimental data for $T_c(x)$ [10] suggests a linear behaviour in the range of x of the order 0.015–0.035 which would imply, through equation (5), a constant p in that range; this constant behaviour, however, should not prevail at low concentrations, $x \to 0$, and presumably one should have $p \propto x \to 0$. For x in the range 0.035–0.07, one may choose to interpolate the theoretical data points through a smooth curve to guide the eye. These considerations lead to the full curve displayed in figure 1, which lies within the error bars of the calculated hole concentrations.

Our theoretical estimates for $p(x)$ are therefore strongly suggestive of $p(x)$ reaching a maximum value within the metallic phase. As a consequence, all attempts to increase T_c should be carried out for samples in the metallic phase, for Mn concentrations about 0.05. Moreover, notwithstanding the considerable uncertainties[4] in the measurements of p, the data shown in figure 1 are in qualitative agreement with those obtained from Hall measurements by Matsukura *et al* [11]; as we discuss below, this is also consistent with findings from recent photoemission spectroscopy measurements [23].

At this point several comments are in order. First, the model is indeed very simple, for it does not incorporate aspects such as a Kohn–Luttinger treatment of the valence states [13, 24], effects of impurity potentials, a site energy term arising from the Mn potential, a correlation energy representing hole–hole repulsion, and so forth. In addition, the model is treated within a mean-field approximation which neglects fluctuations in spin, charge, and disorder degrees of freedom. Nonetheless, one expects these limitations to be minimized, to some extent, by the fact that experimental data for $T_c(x)$ are used as input. However, it is exactly this simplicity that allows us to obtain *a direct* relation between hole concentration and Mn fraction, which, in turn, can be promptly used as a rough guide to experiments. Clearly, the present results must be viewed as a first approximation to $p(x)$, since one should still be able to obtain such a relation phenomenologically through improved models and approximations, though with a considerable amount of extra computational effort. Consider, for instance, the case of Monte Carlo simulations of the Kohn–Luttinger Hamiltonian for the semiconductor valence bands [25]: since the dependence of T_c on J_{pd} and on m^* is different from that of the mean-field prediction (equation (4)), the one-parameter fitting strategy adopted here is not so straightforwardly applicable; these parameters would have to be separately adjusted, demanding many additional runs. It is therefore hardly surprising that most of the improved theoretical approaches [13, 25–27] consider p (instead of x) as an independent variable and, accordingly, present plots of $T_c(p)$, *for fixed x*; the issue of the relation between p and x is then set aside.

The present approach also leads to a qualitative understanding of the x-dependence of p as being essentially related to the occurrence of MITs taking place in the hole subsystem. Within our approximation, the Fermi energy tracks the behaviour of p, since $\varepsilon_F \propto p^{2/3}$, while the exchange splitting $\Delta \propto x$. Figure 2(*a*) shows the schematic impurity bands for each spin

---

[4] For instance, figure 2 of [11] indicates that for $x = 0.022$, the experimentally determined p has an error bar which covers over one decade, while for $x = 0.071$ the error bar runs over two decades.
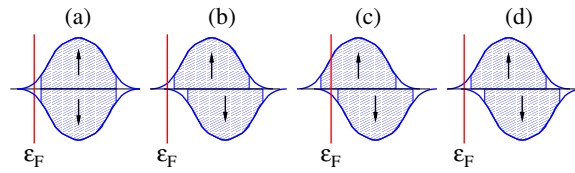
Figure 2. A schematic diagram of the density of states (DOS) versus the energy for the impurity band, for up spins (top) and down spins (bottom). Under each DOS curve, the hashed and empty regions correspond, respectively, to delocalized and localized states; these are separated by mobility edges. The exchange splitting is proportional to the offset between the ↑ and ↓ bands, and the Fermi energy (ε_F) increases to the right, towards the top of the valence band (not shown).
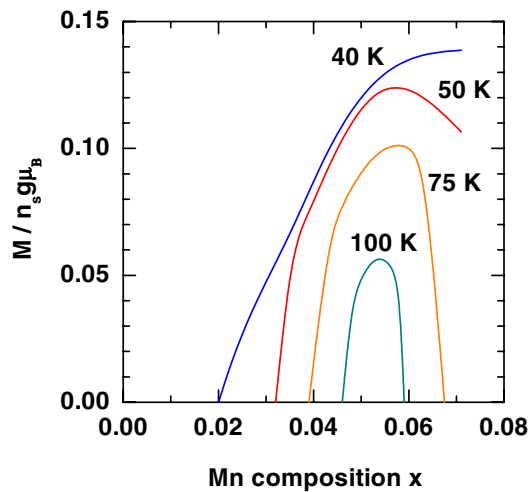

Figure 3. The Mn contribution to the magnetization (equation (2)) as a function of the fraction of Mn sites, for four different temperatures, $T = 40$, 50, 75, and 100 K.

channel, in the very-low-doping regime in which the gas is supposed to be unpolarized. As x increases, the gas can sustain polarization and still be insulating, provided that the Fermi energy lies below the mobility edge, as shown in figure 2(*b*). Further increase in x causes ε_F to increase and to lie within the delocalized states of the up-spin impurity band, as depicted in figure 2(*c*): the system becomes metallic. Whether or not the Fermi energy also lies within the delocalized region of down-spin impurity band is a very interesting question, which cannot be answered by our simple model; the solution of this particular issue should have bearings on the efficiency of $Ga_{1-x}Mn_xAs$-based devices as spin filters. Once ε_F reaches a maximum within the metallic phase, its initial decrease upon increasing x is compensated by an increase in Δ, so the Fermi level still lies within the delocalized states. However, with continuing increase in x the exchange splitting can no longer make up for the decrease in ε_F, and the latter eventually crosses the mobility edge again, then lying within localized states (figure 2(*d*)): the system re-enters an insulating phase. One may argue that a description in terms of *impurity levels* rather than *impurity bands* may be more appropriate in the range of Mn concentrations considered here. Even so, the movement of the Fermi energy described above is still applicable with slight modifications: the metallic phase would then correspond to ε_F reaching the top of the valence band. This latter picture is actually in qualitative agreement with recent photoemission measurements [23] of the Fermi level as a function of Mn concentration in $Mn_xGa_{1-x}As$.

We now discuss the magnetization of the Mn ions, as obtained by solving equations (2) and (3) for M for a given Mn composition and temperature. The mean-field theoretical results are shown in figure 3 for various temperatures; for $T = 75$ and 100 K, we had to resort to an interpolation of the experimental T_c data from Ohno and Matsukura [10]. Two effects are apparent from the calculated results. Firstly, the magnetization maxima with respect to x decrease with increasing temperature, as would be expected, since one approaches the critical temperature from below (see also figure 3(c) of [10]). Moreover, the widths of the composition-dependent magnetization curves decrease quite dramatically with temperature. An immediate consequence of these results is that DMS (Ga, Mn)As device applications at temperatures $\lesssim T_c$ would require definite quality control of the Mn doping level.

In summary, we have established a theoretical scenario for the behaviour of the hole concentration in $Mn_xGa_{1-x}As$ as a function of both x and T_c, based on a simple mean-field approximation to the hole-mediated ferromagnetic Hamiltonian. In our picture, the concentration of holes is approximately constant in the low-doping insulating phase, then rises to a maximum in the metallic phase, and drops again in the re-entrant insulating phase. Our approach also allows one to view the underlying mechanism of the re-entrant MITs as an oscillation of the Fermi energy caused by a delicate balance between band filling and exchange splitting. We have also noted that the larger the temperature, the narrower the range of compositions leading to a non-zero Mn magnetization. The present approach should certainly be extended to include a more complete description of the acceptor states, taking into account the spin degrees of freedom, spin–orbit coupling, compressive/tensile strains, etc. Moreover, a proper treatment of disorder—e.g., by explicitly considering a random, instead of continuous, distribution of Mn ions—should lead to a more realistic description of the MIT. In this respect, many-body effects due to correlation among the holes should also influence $p(x)$, especially in the insulating phase. Of course, giving an appropriate description of the physical mechanisms related to As antisites and Mn^{6As} centres, as far as the hole versus Mn concentrations is concerned, is certainly a formidable task, which nonetheless deserves future theoretical attention.

Acknowledgments

References

[1] Ohno H, Munekata H, Penney T, von Molnár S and Chang L L 1992 *Phys. Rev. Lett.* **68** 2664
[2] Ohno H, Shen A, Matsukura F, Oiwa A, Endo A, Katsumoto S and Iye Y 1996 *Appl. Phys. Lett.* **69** 363
[3] Ohno H 1998 *Science* **281** 951
[4] Flederling R, Kelm M, Reuscher G, Ossau W, Schmidt G, Waag A and Molenkamp L W 1999 *Nature* **402** 787
[5] Ohno Y, Young D K, Beschoten B, Matsukura F, Ohno H and Awschalom D D 1999 *Nature* **402** 790
[6] Ohno H 1999 *J. Magn. Magn. Mater.* **200** 110
[7] Dietl T, Ohno H, Matsukura F, Cibert J and Ferrand D 2000 *Science* **287** 1019
[8] DiVincenzo D P 1999 *J. Appl. Phys.* **85** 4785
[9] Hayashi T, Tanaka M and Nishinaga T 1997 *J. Appl. Phys.* **81** 4865
[10] Ohno H and Matsukura F 2001 *Solid State Commun.* **117** 179
[11] Matsukura F, Ohno H, Shen A and Sugawara Y 1998 *Phys. Rev.* B **57** R2037
[12] Szczytko J, Mac W, Twardowski A, Matsukura F and Ohno H 1999 *Phys. Rev.* B **59** 12 935
[13] Dietl T, Ohno H and Matsukura F 2001 *Phys. Rev.* B **63** 195205

[14] Look D C 1991 *J. Appl. Phys.* **70** 3148
[15] Van Esch A, Van Bockstal L, De Boeck J, Verbanck G, van Steenbergen A S, Wellmann P J, Grietens B, Bogaerts R, Herlach F and Borghs G 1997 *Phys. Rev.* B **56** 13 103
[16] Dietl T, Haury A and Merle d'Aubigné Y 1997 *Phys. Rev.* B **55** R3347
[17] Jungwirth T, Atkinson W A, Lee B H and MacDonald A H 1999 *Phys. Rev.* B **59** 9818
[18] Lee B, Jungwirth T and MacDonald A H 2000 *Phys. Rev.* B **61** 15 606
[19] Hong S P, Yi K S and Quinn J J 2000 *Phys. Rev.* B **61** 13 745
[20] König J, Lin H-H and MacDonald A H 2000 *Preprint* cond-mat/0010471
[21] Litvinov V I and Dugaev V K 2001 *Phys. Rev. Lett.* **86** 5593
[22] Ohno H, Matsukura F, Omiya T and Akiba N 1999 *J. Appl. Phys.* **85** 4277
[23] Asklund H, Ilver L, Kanski J and Sadowski J 2001 *Preprint* cond-mat/0112287
[24] Abolfath M, Jungwirth T, Brum J and MacDonald A H 2001 *Phys. Rev.* B **63** 054418
[25] Schliemann J, König J and MacDonald A H 2001 *Phys. Rev.* B **64** 165201
[26] Chattopadhyay A, Das Sarma S and Millis A J 2001 *Phys. Rev. Lett.* **87** 227202
[27] Jungwirth T, Lee B and MacDonald A H 2001 *Physica* E **10** 153